

A π -Stacked Organometallic Propeller: Experimental and Theoretical Studies on Reactivity and Bonding in the π -Arene-Bridged Nickel Triple-Decker $\{[(\eta^5\text{-Me}_4\text{EtC}_5)\text{Ni}]\}_2(\mu\text{-}\eta^3\text{:}\eta^3\text{-decacyclene})\}$

Jörg J. Schneider,^{*[a][†]} Dirk Spickermann,^[a] Dieter Bläser,^[a] Roland Boese,^[a]
Paul Rademacher,^[b] Thomas Labahn,^[c] Jörg Magull,^{[c][††]} Christoph Janiak,^{[d][†††]}
Naka Seidel,^[e] and Klaus Jacob^[e]

Dedicated to Prof. H. G. Schnöckel on the occasion of his 60th birthday

Keywords: Sandwich complexes / Nickel / Arenes / EHMO calculations / Cyclopentadienyl ligands

Synthesis, structure, reactivity, and theoretical studies of a new type of Ni triple-decker complexes are reported. A prominent feature of its molecular structure is the $(\eta^3\text{:}\eta^3)$ -bis-(enyl) coordination of two $[(\eta^5\text{-Me}_4\text{EtC}_5)\text{Ni}]$ fragments to the central arene ring of the polycondensed π -perimeter decacyclene. The central arene ring of decacyclene displays a distinct chair conformation with significant tilt angles of 25.5 and 26.1°. The three naphthalene units are twisted in a propeller-like fashion with torsion angles of 16°, 16.6°, and 19°, which is twice the twisting observed for the free decacyclene ligand. According to Extended Hückel Molecular Orbital (EHMO) calculations, a qualitative measure for arene lability in the title compound and a number of related arene-bridged metal complexes can be attributed to a subsequent filling of

metal–arene antibonding orbitals. The experimentally observed reactivities of π -arene exchange in these complexes are reproduced nicely by the EHMO calculations. The title compound offers access to a number of organonickel chalcogenato complexes under mild conditions by cleavage of the S–S, Se–Se, or Te–Te bonds of diorganyl dichalcogenides R–E–E–R. The title compound is also capable of $\text{C}_{\text{sp}^2}\text{-H}$ activation of azobenzene and [(dimethylamino)methyl]ferrocene resulting in orthometallated complexes containing five-membered metallacycles. PES and semi-empirical ZINDO/S calculations were used to study the product of the orthometallation of the title compound with azobenzene. These studies reveal that the HOMO of the metallacycle (IE = 6.45 eV) has dominant Ni–C_{aryl} π -antibonding character.

Introduction

Recently we reported on the first binuclear transition metal complexes of decacyclene containing this large condensed π -perimeter,^[1] whose organometallic chemistry is still virtually unexplored, probably owing to its low solubility.^[2] During the course of our studies of this π -perimeter we have found that two $[(\eta^5\text{-Me}_5\text{C}_5)\text{Ni}]$ fragments are able to coordinate in a triple-decker fashion to decacyclene.^[1] At

that time our findings were based exclusively on the analysis of the characteristic NMR spectroscopic data, which suggest a highly symmetrical coordination mode of the two $[(\eta^5\text{-Me}_5\text{C}_5)\text{Ni}]$ fragments to decacyclene, and steric arguments were put forward in favor of an antarafacial coordination of the two M–L fragments.^[1]

Herein we report on the molecular structure, reactivity, and theoretical studies of the unusual arene-bridged nickel triple-deckers **3** and **4** and their reaction products from reductive cleavage and cyclometallation reactions. A remarkable feature of **3** and **4** are their high capability for controlled release of 15e^- - $[(\text{C}_5\text{R}_5)\text{Ni}]$ fragments under mild conditions. Although triple- and multiple-deckers with nickel constitute a most intriguing class of organometallic compounds,^[3] such an unusual coordination as in **3** and **4** paired with a high reactivity of a π -coordinated middle deck is a rare case.

Results and Discussion

We found that reaction of $[(\eta^5\text{-Me}_4\text{EtC}_5)\text{Ni}(\text{acac})]$ (**1**) with the decacyclide dianion produces the title compound **3** in 74% yield as brown to black crystals [Equation (1)].

^[a] Institut für Anorganische Chemie, der Universität–GH Essen,

Universitätsstraße 5–7, 45117 Essen, Germany
^[b] Institut für Organische Chemie der Universität–GH Essen, Universitätsstraße 5–7, 45117 Essen, Germany

^[c] Institut für Anorganische Chemie der Universität Göttingen, Tammannstraße 4, 37077 Göttingen, Germany

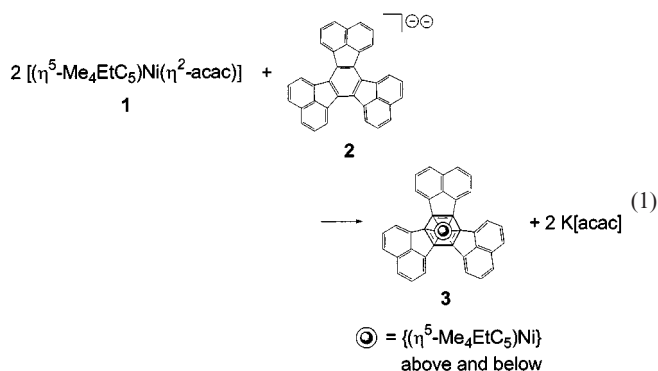
^[d] Institut für Anorganische und Analytische Chemie der Universität Freiburg, Albertstraße 21, 79104 Freiburg, Germany

^[e] Institut für Anorganische Chemie, Martin Luther-Universität Halle-Wittenberg, 06099 Halle/Saale, Germany

^[†] New address: Institut für Chemie, Anorganische Chemie, Universität Graz, Schubertstraße 1, 8010 Graz, Austria, Fax: (internat.) + 43-316/380-9835, E-mail: joerg.schneider@uni-graz.at

^[††] X-ray crystallography.

^[†††] Theoretical calculations.



As for the Me_5C_5 derivative **4**,^[1] the NMR spectra of **3** are characteristic for a symmetric coordination of two $[(\eta^5\text{-Me}_4\text{EtC}_5)\text{Ni}]$ fragments to the decacyclene bridging unit. A high-field coordination shift of the three multiplets (doublet-triplet-doublet) of decacyclene is observed in agreement with a twofold metal coordination to the tris(annulated) center arene ring of decacyclene. However, from NMR experiments on **3** (as for **4**)^[1] no distinction between either a symmetric or an asymmetric metal coordination to decacyclene could be made. For supra- and antarafacial complexes containing bridging arenes highly fluxional behavior is well known. However, low-temperature NMR measurements to prove such fluxional behavior for **3** and **4** are precluded by their low solubility. So far, no decision towards the fluxionality and subsequently the hapticity of **3** and **4** in solution could be made. However, we believe **3** and **4** to be highly fluxional in solution.

In contrast to **4**, the Me_4EtC_5 derivative **3** gave suitable crystals for an X-ray structure determination, which allow us to determine its molecular structure in the solid state (Figure 1).^[4]

The two $[(\eta^5\text{-Me}_4\text{EtC}_5)\text{Ni}]$ fragments of **3** display an η^3 -enyl bonding in which both metal ligand fragments are bonded in an antarafacial fashion to the central benzene ring of decacyclene (Figure 2). This causes the distortion of the central ring into a chair conformation in which the plane defined by $\text{C}^1\text{-C}^2\text{-C}^3$ is tilted by 25.5° , and the plane defined by C^4 , C^5 , and C^6 is tilted by 26.1° towards the plane C^3 , C^4 , C^6 , C^1 . The $\eta^3:\eta^3$ coordination in **3** has some precedent in the literature when considering polynuclear arenes as bridging ligands (Figure 3).^[5–8] However, **3** represents a rare case in which two Ni ligand fragments are coordinated to a single C_6 arene ring.^[9]

In **3** both Ni atoms are equally displaced between the bridging η^3 -bonded arene part of decacyclene (1.72 \AA) and the $\eta^5\text{-Me}_4\text{EtC}_5$ ligands (1.73 \AA). As a result of the antarafacial $\eta^3:\eta^3$ coordination, a substantial twist of the mean planes of the crystallographically independent naphthalene moieties of 16° , 16.6° , and 19° results. This exceeds the modest twist disposed on the naphthalene moieties of the free ligand by almost 100% (9.3° and 7.7°) and gives **3** a distinct propeller-like shape when compared to free decacyclene (see Figure 2).^[10]

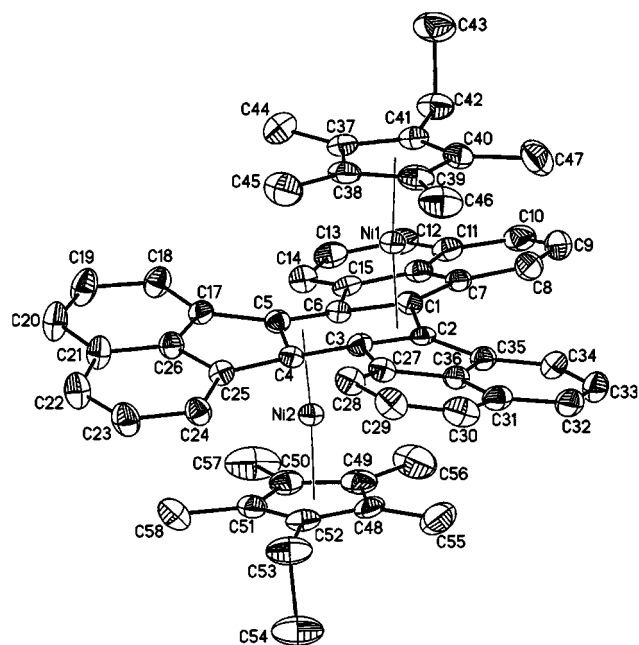


Figure 1. Molecular structure of **3** as determined in the solid state; selected bond lengths [Å] and angles [$^\circ$]: $\text{C}^1\text{-C}^2$ 1.445(6), $\text{C}^1\text{-C}^6$ 1.513(6), $\text{C}^1\text{-C}^7$ 1.472(6), $\text{C}^2\text{-C}^3$ 1.453(6), $\text{C}^2\text{-C}^{35}$ 1.465(6), $\text{C}^3\text{-C}^4$ 1.484(6), $\text{C}^3\text{-C}^{27}$ 1.483(6), $\text{C}^4\text{-C}^5$ 1.482(6), $\text{C}^4\text{-C}^{25}$ 1.488(6), $\text{C}^5\text{-C}^6$ 1.415(6), $\text{C}^5\text{-C}^{17}$ 1.475(6); $\text{C}^1\text{-C}^6\text{-C}^2$ 119.5(4), $\text{C}^3\text{-C}^4\text{-C}^2$ 120.4(4), $\text{C}^4\text{-C}^5\text{-C}^3$ 118.6(4), $\text{C}^5\text{-C}^6\text{-C}^4$ 112.6(4), $\text{C}^6\text{-C}^5\text{-C}^1$ 121.3(4)

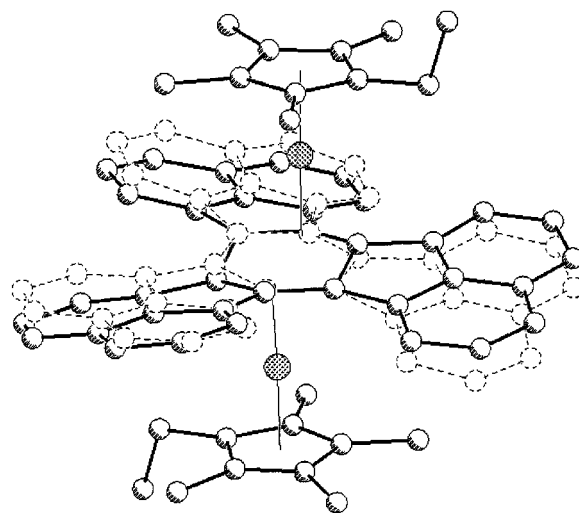


Figure 2. Overlay of the molecular structure of uncomplexed decacyclene **1** and the dinickel triple-decker **3** showing the propeller-like arrangement of the naphthalene units of uncomplexed **1** and the bridging decacyclene ligand of **3**; atom numbering scheme according to Figure 1

Reactivity Studies of **3** and **4**

The decacyclene ligand in **3** and **4** can be displaced, resulting in the formation of dinuclear and mononuclear organonickel complexes. Common features of all exchange reactions are the mild reaction conditions (room temperature) and the possibility of the immediate visual progress of the ligand exchange by appearance of a precipitate of highly

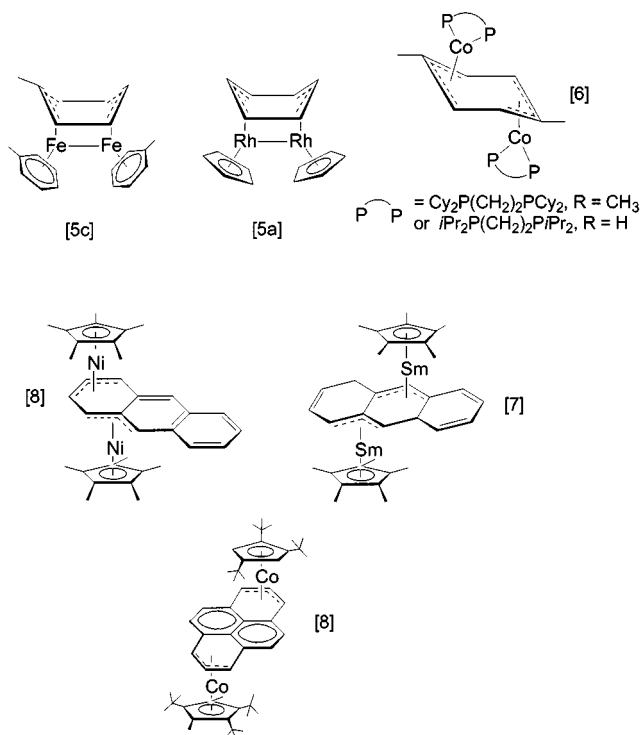


Figure 3. Selection of dinuclear complexes containing polynuclear arenes as bridging ligands

insoluble decacyclene **2**. This lability of the aromatic middle deck make **3** and **4** ideal, and so far rare sources for the mild in situ generation of $15e^- - [(\eta^5-C_5R_5)Ni]_{solv}$ fragments with a high synthetic potential in organometallic synthesis. To the best of our knowledge, no other comparable sources for $[(\eta^5-C_5R_5)Ni]_{solv}$ fragments are known so far.

Reactions of **3** with Diphenyl Disulfide (**5**), Dimesityl Diselenide and Ditelluride (**6** and **7**), and Dinaphthyl Ditelluride (**8**) – Formation of (μ -Chalcogenato)dinickel Complexes **9–12**

Diorganyl dichalcogenides are prone to homolytic cleavage of the E–E bond by transition metal ligand fragments, which generate reactive R–E fragments. Related oxidative additions of acyclic organic, cyclic organic, and organometallic dichalcogenides are also known.^[11] Organonickel thiolate complexes are possible reaction products from cleavage reactions of R–S–S–R compounds. They are often electrochemically active but show a pronounced stability towards one-electron reduction and cleavage of their M–S bond(s).^[12]

Our interest in binary and ternary transition metal chalcogen complexes and their electron-transfer properties^[13] prompted us to study the reaction of **3** with dichalcogenides **5–8** with respect to a transfer of $15e^- - [(\eta^5-Cp^R)Ni]$ fragments.

Addition of a stoichiometric amount of the appropriate diorganyl dichalcogenide to a solution of **3** in diethyl ether resulted in the precipitation of decacyclene as a tan-colored powder. The chalcogenato complexes **9–12** could be isol-

ated in high yields from the filtered solution [Equation (2)]. The formation of **9–12** can be understood by reductive cleavage of the E–E bond of the dichalcogenide by reactive $[(\eta^5-Me_4EtC_5)Ni]$ fragments.

Dinuclear complexes of general type $\{[(\eta^5-C_5R_5)Ni(\mu-ER)]_2\}$ can exist in planar or bent conformations with regard to the Ni_2E_2 core.^[14] Varying substituents at the bridging chalcogen atoms S, Se, and Te may cause the Ni_2E_2 core to adopt different orientations, reflecting different hybridization situations at the chalcogen atoms (Figure 4).

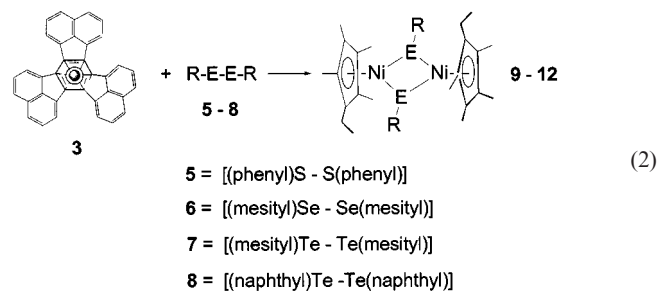


Figure 4. Possible conformations for complexes of the type $\{[(\eta^5-Cp^R)Ni(\mu-SR)]_2\}$

Despite this possibility, the 1H NMR spectra of the complexes **9–12**, show the presence of only one conformer. However, for $\{[(\eta^5-Me_4EtC_5)Ni]_2(\mu-SeMes)_2\}$ (**10**), unusually broad signals in the 1H NMR might indeed indicate a dynamic behavior of this compound in solution.

The molecular structure of bis[(μ -benzenethiolato)($\eta^5-Me_4EtC_5$)Ni] (**9**) in the solid state was confirmed by X-ray crystallography and revealed two independent molecules. However, no significant variation in bonding parameters was observed.^[4] Each molecule of **9** has a centrosymmetric structure with a nearly square-planar Ni_2S_2 arrangement (Figure 5). The distances between the two nickel atoms are 3.078 Å ($Ni-Ni'$) and 3.109 Å ($Ni-Ni''$; not shown), which is obviously too large to consider Ni–Ni metal bonding when compared to the Ni–Ni distance of 2.4916 Å in metallic Ni.^[15] Other bonding parameters for **9** are in close agreement to those in bis[($\eta^5-C_5H_5$)Ni($\mu-S$ -phenyl)].^[12] Due to the diamagnetic nature of **9–12** the two sulfur atoms have either the formal oxidation state +2 or +4 giving the two nickel centers a $16e^-$ or $18e^-$ count in these complexes.

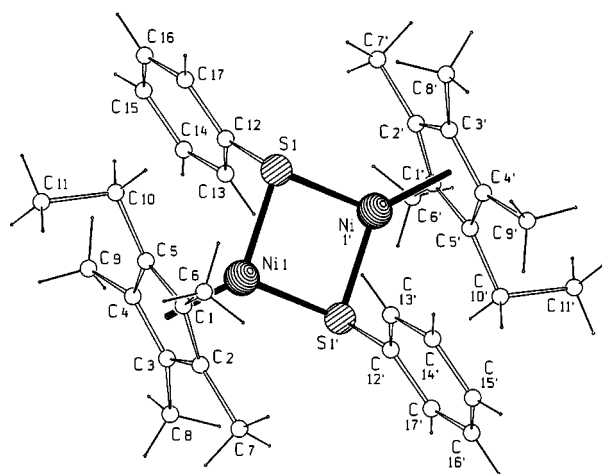


Figure 5. Molecular structure of **9** [only molecule **9**(1) is shown] as determined in the solid state; selected bond lengths [Å] and angles [°] of **9**(1): Ni¹–S¹ 2.194(2), Ni¹–S¹ 2.198(4); Ni¹–S¹–Ni¹ 89.00(6), S¹–Ni¹–S¹ 91.00(6)

Reactivity Studies

C_{sp²}–H-Activation of Azobenzene and [(Dimethylamino)methyl]ferrocene

Orthometallation reactions involving C_{sp²}–H bond activation processes represent an important class of reactions with various examples exemplified in the recent literature.^[16] From a preparative point of view, transmetallation is a rather attractive preparative route that offers access to orthometallated complexes containing pseudoaromatic rings.^[17] During the course of our studies, we have found that **3** and **4** are able to undergo C_{sp²}–H orthometallations with achiral and prochiral aromatic ring systems under mild conditions by transfer of the [(η⁵-Cp^R)Ni] (R = Me₅, EtMe₄) moiety.

Reaction of **3** and **4** with Azobenzene

Nickelocene undergoes an orthometallation reaction with azobenzene at high temperatures, leading to a blue crystalline product formulated as [(η⁵-Cp){(*o*-phenylazo)phenyl}Ni].^[18] In addition, cyclopalladation reactions have been reported for a couple of substituted azobenzenes.^[16a,19,20] The palladium–carbon bond is preferentially formed with the benzene ring bearing the electron-donating group, thus pointing towards the electrophilic character of the cyclopalladation reaction.^[16a]

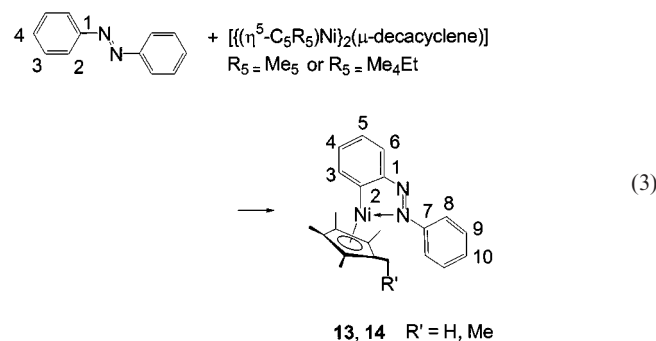
Addition of a twofold excess of azobenzene to a solution of **3** or **4** in diethyl ether gives an intense bright blue solution within minutes, accompanied by precipitation of solid decacyclene as tan-colored powder. Deep blue to black, air stable crystals of **13** and **14** could be isolated therefrom [Equation (3)]. The mass spectra of **13** and **14** display the corresponding molecular peaks as base signal, thus establishing a 1:1 ratio azobenzene/[(η⁵-C₅R₅)Ni] for both complexes. The ¹H NMR spectrum of **13** gives clear evidence of one [(η⁵-Me₄EtC₅)Ni] fragment asymmetrically bonded

to the azobenzene moiety as a result of an orthometallation reaction. The signal of the α-proton of the metallated phenyl ring is shifted downfield to δ = 7.86 compared to free azobenzene (Δδ = –0.4). Similar ¹H NMR coordination shift effects have been observed e.g. for orthometallated pyridine.^[21]

The ¹³C NMR spectrum of **13** shows a characteristic downfield shift for the metallated carbon atom (C²) compared to free azobenzene (Δδ = –59.2) well in accordance with the ¹H NMR spectrum.

The signals of the neighboring carbon atoms C¹ and C³ are shifted 10 ppm down-field compared to those of free azobenzene. All other carbon resonances do not show significant and characteristic coordination shifts upon Ni coordination. The NMR spectroscopic data of **14** are in agreement with those of **13** (see Exp. Sect.).

Unfortunately, an X-ray crystal-structure analysis of **13** suffers from intense disorder of the EtMe₄C₅ ligand. However, the connectivities of all atoms except hydrogen could be unambiguously pinpointed from the crystallographic data set, thus surely confirming the existence and coordination of the orthometallated five-membered nickelabenzpyrazole ring, as it is shown in Equation (3). The (Cp)nickel moiety coordinates to the nitrogen atom of the diazo group via its lone pair, thus allowing the Ni center to attain an 18e[–] count.



Corresponding to its elusive bright blue color, the relevant absorption for **13** is found at λ = 609 nm (ε = 6317) (Figure 6). The characteristic absorptions for the azobenzene residue are shifted to higher wavelengths compared to those of free azobenzene. The same effect is observed for the absorptions of the parent corresponding [(*o*-(phenylazo)phenyl)(η⁵-Cp)Ni] complex^[18] and for [(*o*-(phenylazo)phenyl)PtCl₂]₂,^[19] both containing five-membered orthometallated ring systems incorporating the N=N azo group. It is interesting to note that differently alkyl-substituted *o*-hydroxyazobenzene compounds experience a similar bathochromic shift compared to azobenzene resulting in a blue to purple color as observed for **13** and **14**.^[22] The effect is attributed to hydrogen bonding of an *o*-OH group to the nitrogen atom of the azo group, resulting in formation of six-membered rings and the term *internal halochromism* has been coined for it.^[22]

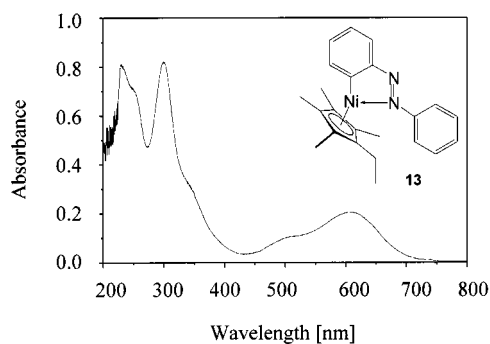


Figure 6. UV/Vis spectrum of **13** in CH_2Cl_2 (27 °C)

In contrast with the reaction of nickelocene with azobenzene, which requires drastic reaction conditions and prolonged reaction times to proceed to completion, the generation of $15e^- - [(\eta^5\text{-C}_5\text{R}_5)\text{Ni}]$ fragments ($\text{R} = \text{Me}_5, \text{EtMe}_4$) from triple-deckers **3** and **4** undergoing the cyclometallation of azobenzene is already achieved at room temperature within minutes. This suggests that $[(\eta^5\text{-C}_5\text{R}_5)\text{Ni}]_{\text{solv}}$ fragments are easily generated by a dissociative pathway from triple-decker complexes **3** and **4**. A dissociative mechanism for ligand exchange has been proven recently for arene-bridged Co triple-deckers $[(\eta^5\text{-C}_5\text{R}_5)\text{Co}]_2(\mu\text{-}\eta^4\text{:}\eta^4\text{-arene})$ ($\text{R} = \text{Me}_5, 1,2,4$ tri-*tert*-butyl) by kinetic and preparative studies.^[23]

Photoelectron Spectroscopy (PES) of **13**; Experimental and Theoretical Studies

The (He^1) PE spectrum of **13** is shown in Figure 7. Experimental vertical ionization energies are listed in Table 1. The calculated PE spectrum together with relevant MO contributions, obtained from semiempirical ZINDO/S calculations based on the corresponding model compound $[(\eta^5\text{-Cp})\text{Ni}(\text{C}_6\text{H}_4\text{-N=N-C}_6\text{H}_5\text{-}\kappa\text{C,}\kappa\text{N})]$ **A** (simplification of alkyl ligand substituents by hydrogen) is depicted in Figure 8. Zerner (**Z**) et al. have employed an intermediate neglect of differential overlap (INDO) method with spectroscopic parametrization (ZINDO/S) in electronic calculations.^[24] Following this work we have used the semi-empir-

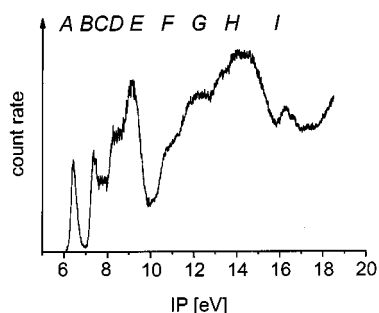


Figure 7. Experimental He^1 PE spectrum of **13**; assignment see Figure 8

ical ZINDO/S method in the calculation of the PE spectrum of **13**.

Table 1. Experimental vertical ionization energies (in eV; ca. 1.60×10^{-19} J) for **14**; for a detailed assignment see text and Figure 8

Band	$IE_{\text{vert.}}$	Assignment
A	6.45	HOMO: π antibonding
B	7.36	
C	7.50	HOMO1 –
	7.81	HOMO5:
D	8.43	π ligand
E	9.12	centered
F	10.77	HOMO6 –
I	16.28	HOMO11

The ionization energies of the nickel compound have been evaluated by Koopmans' theorem^[25] as the negative of the eigenvalues of the ground state MOs of the neutral molecules. We are aware that Koopmans' approximation is often not valid in the case of organo transition metal complexes. Ferrocene, for example, is a well-known case where the breakdown of Koopmans' theorem was demonstrated.^[26] However, the spectroscopic parameterization employed in the INDO/S method resulted in a rather large reduction of relaxation energy and Koopmans' theorem was found to give a correct order of ionization potentials.^[24,27] As can be seen from Figure 7, Figure 8, and Table 1 the energies of the molecular orbitals based on a calculation of the model species **A** deviate less than 1.0 eV from observed ionization potentials. The low molecular symmetry of **A** leads to substantial atomic orbital mixing. This makes an assignment of characteristic molecular orbitals to spectral bands difficult. The band at 6.45 eV is assigned to the HOMO, which is an Ni–Cp and Ni–C_{aryl} π -antibonding orbital. The calculation gives 5 MOs (HOMO-1 to HOMO-5), which are assigned to the region between 7.36 and 9.4 eV. These MOs are dominated by ligand-centered π orbitals. Most prominent are aryl and cyclopentadienyl π sets that contribute significantly to these molecular orbitals (Figure 9). Some nickel d-character is also present, but except for one orbital (HOMO-4/-5) never prominent. There it is part of an Ni–C_{aryl} σ -bonding orbital.

From the HOMO-6 downward, the calculated MOs are assigned to the experimental ionization energy region above 10.7 eV. These not very well resolved bands start with Ni–Cp π -bonding orbitals (HOMO-6, -9) as well as nickel-centered nonbonding d-orbitals (HOMO-7, -8). Some weak Ni–C_{aryl} σ -bonding is also present (HOMO-8, -10). An Ni–N bonding and N-lone-pair combination is calculated around 11.2 eV (HOMO-11).

Reaction of **3** with Bis[2-[(dimethylamino)methyl]-ferrocenyl]lead(II) (**15**)

Due to our continued interest in the synthesis of transition metal complexes containing stannylene species :MR₂

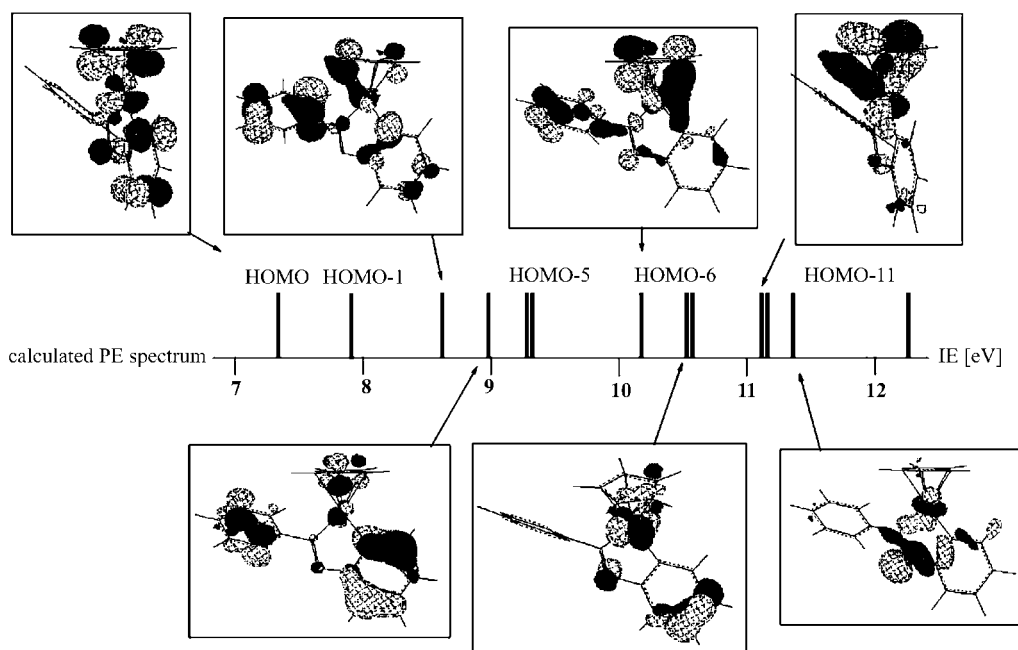


Figure 8. Calculated PE spectrum of **13** together with calculated ZINDO/S MOs assigned to the individual vertical ionization energies

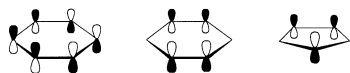


Figure 9. Prominent molecular orbital contributions from aryl and Cp π -sets in the energy window 7.36–9.4 eV

(Sn, Pb)^[28] we studied the complexation behavior of **3** towards the unique intramolecular donor-stabilized plumblylene **15**.^[29] The obvious ease with which $15e^-$ - $[(\eta^5-C_5R_5)Ni]$ fragments could be generated from **3** spurred our interest in the synthesis of new Ni–plumblylene complexes derived from **15**. Complex **15** is a uniquely chelated Pb^{II} compound, which owes its stability to an intramolecular twofold N-donor stabilization (Figure 10).^[33] An intramolecular exchange process is responsible for equivalency of both Fc–N groups in solution, giving rise to temperature- and solvent-dependent equilibrium of *meso/rac* diastereoisomers of **15**.^[29]

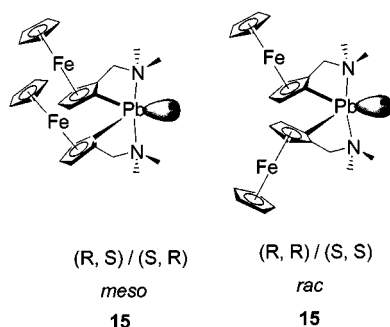
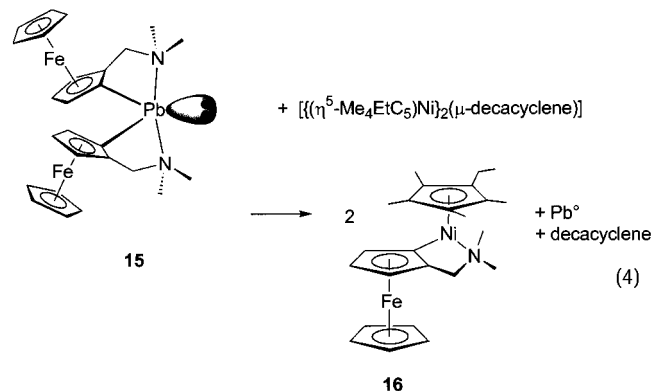


Figure 10. *meso* and *rac* isomer of **15**^[29]

Addition of solid **3** to a yellow suspension of **15** in diethyl ether at -78°C gave a magenta-colored solution, accompanied by immediate elimination of **2** as tan-colored precip-

itate. However, on warming up to ambient temperature the color changed from magenta to red. From this solution (*R,S*)-**16** could be isolated as a racemic mixture, as the only product [Equation (4)]. The cyclometallation of the [(dimethylamino)methyl]ferrocenyl ligand proceeds by a transmetallation reaction of the *meso/rac* diastereomer **15**. The intramolecular N \rightarrow Pb stabilization present in **15** is obviously not sufficient to stabilize a Pb–Ni coordination bond at room temperature. It is obvious that the initially observed magenta color of the reaction mixture is indeed due to formation of a Pb^{II}–Ni species initially formed in the reaction between **3** and **15**. We have found that complexes containing similar Sn^{II}–Co(Fe) bonds do show the same characteristic magenta color; as do initial reaction solutions of **3** and **15**. However, the Sn^{II}–Co(Fe) complexes are fairly stable under ambient conditions.^[29] In contrast, the Pb^{II}–Ni species do not prove to be stable and eliminate Pb⁰, liberating the ferrocenyl ligands, which undergo subsequent orthometallation to give **16**.



In the ^{13}C NMR spectrum the signal of the metallated carbon atom C^2 ($\delta = 103.8$) is shifted by about 35 ppm to lower field compared with that of the nonmetallated Cp ligand of the ferrocene moiety ($\delta = 69.1$), well in agreement with the observations for the azobenzene complexes **13** and **14**. The ^1H NMR spectroscopic data are in close agreement to the related cationic Co^{III} complex $[(\eta^5\text{-C}_5\text{H}_5)\text{Co}(\eta^5\text{-C}_5\text{H}_5)\text{Fe}(\eta^5\text{-C}_5\text{H}_3\text{CH}_2\text{NMe}_2)(\text{PMe}_3)]^+\text{PF}_6^-$ reported recently.^[30]

X-ray Analysis of **16**

Figure 11 depicts the molecular structure of **16** as a result of a single-crystal X-ray diffraction study. As concluded from the NMR spectroscopic data, the $[(\eta^5\text{-Me}_4\text{EtC}_5)\text{Ni}]$ fragment is indeed coordinated to the *o*-carbon atom (C^{10}) and to the nitrogen atom of the [(dimethylamino)methyl]Cp ring of the ferrocene subunit, giving the nickel center a nearly trigonal-planar coordination. The planes of the Me_4EtC_5 ring and the five-membered metallacycle are nearly perpendicular to each other (87.8°) (Figure 12). The Fe distances to the ring centroids of the unsubstituted and the annulated Cp ring of the sandwich unit are equal within experimental error, thus indicating no significant influence of the Ni-chelate ring with respect to bonding in the ferrocene part. The distance $\text{Ni}-\text{Cp}_{\text{centroid}}$ equals that in **16** (1.74 Å). The nickelacycle is slightly puckered as can be seen when viewed along the Ni–N axis (Figure 12). The puckering is related to the torsion angles of the best planes defined by $\text{C}^9\text{-C}^{22}\text{-Ni}$ and $\text{C}^9\text{-C}^{10}\text{-Ni-N}$, which is 11.2° .

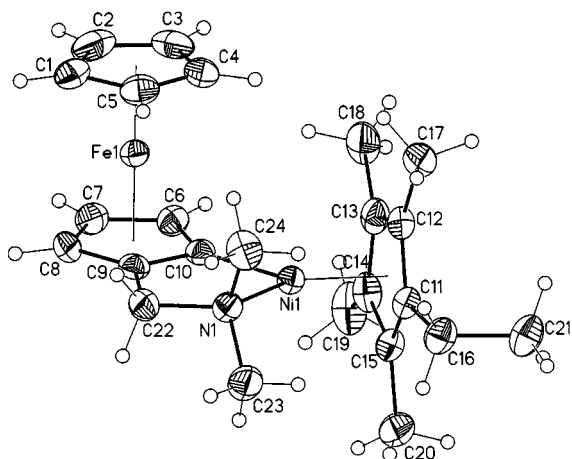


Figure 11. Molecular structure of **16** as determined in the solid state; selected bond lengths [Å] and angles [$^\circ$]: $\text{Ni}^1\text{-C}^{10}$ 1.881(3), $\text{Ni}^1\text{-N}^1$ 2.001(2), $\text{Ni}^1\text{-C}^{22}$ 1.513(3), $\text{C}^{10}\text{-Ni}^1\text{-N}^1$ 86.99(10); $\text{C}^9\text{-C}^{22}\text{-Ni}^1$ 108.9(2), $\text{C}^{22}\text{-Ni}^1\text{-Ni}^1$ 111.13(15)

Theoretical Studies on π -Arene Ligand Lability in Arene-Bridged Triple-Deckers of Co and Ni

An intriguing question regarding the reactivity of the (decacyclene)Ni triple-deckers **3** and **4** is the cause of their un-

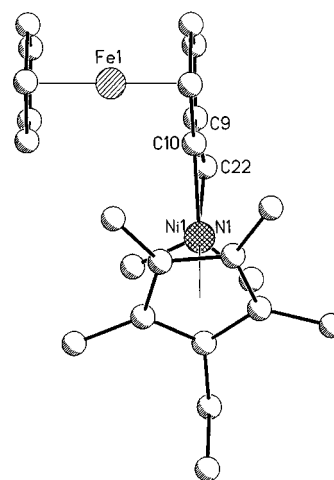


Figure 12. View along the Co–N bond axis of **16**, showing the slight puckering of the metallacycle; atom numbering scheme according to Figure 11

usual arene lability under the mild conditions reported herein. Definite notation of arene lability in binuclear complexes has been reported for only a very limited number of cases so far. Thus, we were interested to see whether calculations on the EHMO level could provide, aside from our experimental studies, theoretical insight into this lability for **3** and **4**. Furthermore, we would like to compare our results with other related di- and mononuclear complexes showing related characteristic behavior towards arene exchange.

In choosing the EHMO approach we hoped to obtain reliable and still interpretable (at least in well-established chemical paradigms) semiquantitative information on this question.

The arene lability in the triple-decker complexes **3** and **4** can be compared to the following triple-decker compounds: (a) $[(\eta^5\text{-C}_5\text{H}_5)\text{V}(\mu\text{-}\eta^6\text{:}\eta^6\text{-C}_6\text{H}_6)\text{V}(\eta^5\text{-C}_5\text{H}_5)]$ ^[31] (arene exchange only above 120°C); (b) $[(\eta^5\text{-C}_5\text{R}_5)\text{Co}(\mu\text{-}\eta^4\text{:}\eta^4\text{-toluene})\text{Co}(\eta^5\text{-C}_5\text{R}_5)]$ ^[23] ($\text{R}_5 = 1,2,4\text{-}t\text{Bu}_3, \text{Me}_5$) (arene exchange at ambient temperature, compound stable in solution at ambient temperature). In addition the following mononuclear complexes are available for comparison: (c) $[(\eta^6\text{-toluene})\text{Ni}(\text{C}_6\text{F}_5)_2]$ ^[32] (arene extremely labile, arene exchange at ambient temperature); (d) $[(\eta^6\text{-toluene})\text{Co}(\text{C}_6\text{F}_5)_2]$ ^[32] (arene extremely labile, arene exchange at ambient temperature); (e) $[(\eta^6\text{-toluene})\text{Fe}(2,2'\text{-bipyridine})]$ ^[33] (arene is not labile); (f) $[(\eta^6\text{-C}_6\text{H}_6)\text{Ni}(\eta^1\text{-}t\text{Bu}_2\text{PCH}_2\text{P-}t\text{Bu}_2)]$ ^[34] (decomposition in solution above -30°C , probably due to M–arene dissociation, e.g. the compound is not stable in solution at ambient temperature, however, between -80 to -30°C no arene exchange was found on the NMR time scale).

From these complexes model compounds were constructed through the simplification of alkyl ligand substituents by hydrogen, i.e. in the calculations only C_5H_5 and C_6H_6 were employed. Calculations were performed on the symmetrical triple-decker complexes **A** [(Figure 13)]. The actual $\eta^3\text{:}\eta^3$ or $\eta^4\text{:}\eta^4$ coordination in the nickel and cobalt triple-deckers was considered by looking at the slipped

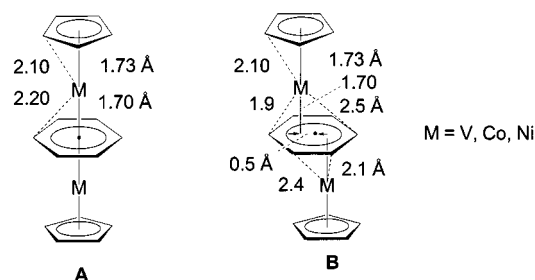


Figure 13. EHMO bonding parameters calculated for the symmetrical (A) and the slipped triple deckers (B)

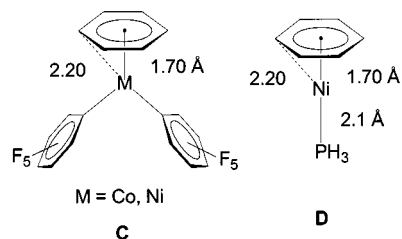


Figure 14. EHMO bonding parameters for the mononuclear complex types C and D

triple-decker complex B. For comparison the mononuclear arene complexes C and D were included in the calculations (Figure 14).

Triple-decker complexes with middle decks other than arenes have been theoretically analyzed before. Theoretical studies are available for sandwich complexes with middle decks such as C_5H_5 ,^[35] P_5 and As_5 , P_6 , P_3 and P_4 .^[36] The orbital interactions of two C_5H_5M fragments with such a middle deck have been well described. In addition, a theoretical study on C is available.^[37] Furthermore, a photoelectron spectroscopic study, and an MO calculation on A with $M = V$ have been carried out.^[38]

As a measure of metal–arene bond stability we have used the concept of overlap population. The Mulliken overlap population between two orbitals located on atoms or fragments X and Y in a molecule is $2c_i c_j S_{ij}$. This corresponds to the amount of electron density transferred to the region between X and Y on interaction of the two orbitals under consideration. Depending on the signs of the orbital coefficients c_i , c_j , the overlap population, representing the shared electron density of X and Y, can be positive or negative. A larger positive overlap population correlates with a stronger bond and a larger bond order between atoms X and Y. However, actual numbers can only be compared within a related series, keeping the atom pair X, Y constant. For example, the overlap population of a transition-metal–transition-metal bond should not be compared to that of a carbon–carbon bond. The orbital overlap (S_{ij}) term is different for different orbitals or atom pairs. Therefore, it is not so much the single, absolute number that is meaningful, but the trend that is observed upon variation of geometrical or electronic factors.^[39,40]

From an Extended Hückel MO study on the model complexes A–D the following situation emerges: Taking the

symmetrical triple-decker A we looked at the M–arene overlap population for $M = V, Co, Ni$ in Figure 15. One has to be cautious about comparing the overlap population for different metals. However, this is not necessary by simulating the variation in metal by the electron count and thereby keeping the atom pairs constant. Starting from the neutral complex for $M = V$ ($26e^-$) and Co ($34e^-$) it is obvious that the M–arene overlap drops when adding additional electrons. Conversely, taking electrons away for $M = Co$ ($34e^-$) and Ni ($36e^-$) increases the M–arene overlap. This can be rationalized by the fact that the frontier orbitals are largely metal-centered, but also with metal-to-ligand antibonding combinations.

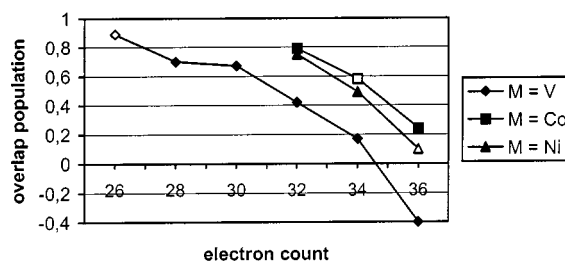


Figure 15. M–arene overlap population in A as a function of electron count (open field \square , \square , Δ is the neutral complex)

Figure 16 compares the M–arene overlap population for the symmetrical and the slipped triple-decker A and B. Upon slippage, the overlap population is slightly lower for $M = V$, but increases considerably for $M = Co$ and Ni . This corresponds to the experimental finding of a symmetrical triple-decker for vanadium and $\eta^3:\eta^3$ or $\eta^4:\eta^4$ slipped sandwiches for cobalt and nickel.

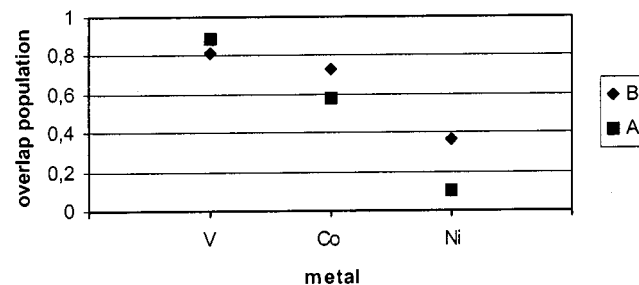


Figure 16. M–arene overlap population in A and B for $M = V, Co$, and Ni (neutral complexes)

As a means of calibration we checked the calculated overlap population towards M–arene overlap populations in the mononuclear complexes C and D with known arene lability. Figure 17 illustrates the results. The overlap population for C is lower than for B with the same metals. This results corresponds nicely to the experimental finding of a rather low activation energy of $10\text{--}11\text{ kcal}\cdot\text{mol}^{-1}$ for arene exchange in C ($M = Ni$),^[32] thus establishing a slightly higher reactivity for arene exchange for C compared to B. For D the overlap population is the lowest within the nickel series. The low overlap population in D compared with B or C ($M = Ni$) was surprising, because no arene exchange was reported by NMR techniques for D. A closer look re-

vealed, however, that $[(\eta^6\text{-C}_6\text{H}_6)\text{Ni}(\eta^1\text{-}t\text{Bu}_2\text{PCH}_2\text{P}t\text{Bu}_2)]^{[34]}$ was reported to be stable in solution only up to $-30\text{ }^\circ\text{C}$. Above that temperature decomposition took place, probably due to M–arene bond dissociation. Hence, NMR exchange studies were not carried out under ambient conditions as for the other compounds but only at temperatures between -80 and $-30\text{ }^\circ\text{C}$, and probably not for an extended period of time.^[34] Hence, the instability of $[(\eta^6\text{-C}_6\text{H}_6)\text{Ni}(\eta^1\text{-}t\text{Bu}_2\text{PCH}_2\text{P}t\text{Bu}_2)]$ is well reflected in the low M–arene overlap population of **D**.

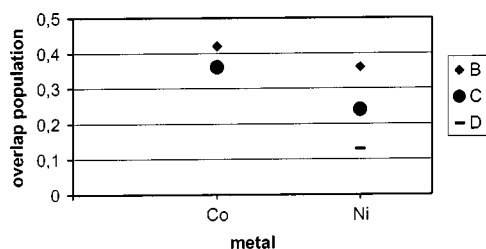


Figure 17. M–arene overlap population in **B**, **C** (M = Co, Ni), and **D**

For useful preparative purposes a labile, yet stable enough character of the M–arene bond is crucial. This results in the combination of two important factors: the ease of handling under ambient conditions, in connection with a still high reactivity for arene exchange under these same conditions. Complexes of type **B** and **C** ideally offer both prerequisites.

Conclusions

Reaction of $[(\eta^5\text{-EtMe}_4\text{C}_5)\text{Ni}(\eta^2\text{-acac})]$ with the dianion of decacyclene resulted in the formation of the slipped triple-decker **3** with a unique antarafacial bis(η^3 -enyl)nickel coordination in the solid state as revealed by X-ray crystallography. Complex **3** and its Me_5C_5 derivative **4** display a high reactivity towards ligand loss. This fact has been proven by formation of a number of organonickel chalcogenato complexes of type $[(\eta^5\text{-Me}_4\text{EtC}_5)\text{Ni}_2(\text{ER})_2]$ (E = S, Se, Te; R = Ph, Mes, Naphth) that are formed by ligand displacement of the polynuclear aromatic middle deck decacyclene. Reaction of **3** and **4** with azobenzene under ligand exchange resulted in $\text{C}_{\text{sp}^2}\text{-H}$ activation of the *ortho* ring position giving a remarkable stable five-membered nickelacycle. Complex **3** reacts with the plumblylene **15** in a transmetallation reaction by elimination of Pb^0 , giving **16**, which contains a cyclometallated ferrocenyl moiety.

The overlap population from EHMO calculations can be used as a qualitative measure for arene lability in metal–arene complexes. Results obtained from these calculations explain the variation of arene lability in this class of compounds. The increased metal–arene lability observed in cobalt and nickel complexes is due to a filling of metal–arene antibonding orbitals.

Experimental Section

General Information: All reactions were carried out under nitrogen using Schlenk techniques; all solvents were dried properly and distilled under appropriate conditions before use. They were stored under nitrogen prior to use. Products were purified by crystallization. Yields refer to analytically pure samples. Decacyclene (Aldrich) was sublimed in vacuo prior to use. Dichalcogenides R-E-E-R were synthesized according to the literature.^[41] NMR spectra were measured at $25\text{ }^\circ\text{C}$ with a Bruker AMX300 or AMX500 and referenced against the deuterated solvents used; coupling constants are given in Hz. NMR samples were prepared by vacuum transfer of dried degassed solvents onto the appropriate amount of solid sample, followed by flame sealing of the NMR tube. MS spectra were recorded with a MAT 8200 instrument using standard conditions (EI, 70 eV) and the fractional sublimation technique for compound inlet. UV/Vis spectra were recorded with a Varian Cary 100 spectrometer under air in 10-mm thick cuvettes. Microanalyses were performed by the microanalytical laboratory of the Chemistry Department of the University–GH Essen.

Photoelectron Spectroscopy Studies (PES): PE spectra were recorded with a Leybold Hereaus UPG200 spectrometer equipped with an He^I radiation source (21.21 eV). Samples were evaporated directly into the target chamber. In order to maintain sufficient vapor pressure of **13** a temperature of $200\text{ }^\circ\text{C}$ was used. The energy scale was calibrated with xenon (12.130 and 13.436 eV) and argon (15.759 and 15.937 eV). The accuracy of the measurements was $\pm 0.03\text{ eV}$ for ionization energies, for broad and overlapping signals $\pm 0.1\text{ eV}$.

Theoretical Studies: Qualitative MO computations were performed within the extended Hückel formalism^[42] with weighted H_{ij} values^[43] with the CACAO program (Version 4.0).^[44] Geometrical parameters were taken from X-ray structural studies of the parent compounds^[3,23,31,33,35] and averaged. For comparison, the same structural parameters were employed for the different metals in the model compounds $[(\eta^5\text{-C}_5\text{H}_5)\text{M}(\mu\text{-}\eta^6\text{-C}_6\text{H}_6)\text{M}(\eta^5\text{-C}_5\text{H}_5)]$ (A: M = V, Co, Ni), $[(\eta^5\text{-C}_5\text{H}_5)\text{M}(\mu\text{-}\eta^3\text{-}\eta^3\text{-C}_6\text{H}_6)\text{M}(\eta^5\text{-C}_5\text{H}_5)]$ (B: M = V, Co, Ni), $[(\eta^6\text{-C}_6\text{H}_6)\text{M}(\text{C}_6\text{F}_5)_2]$ (C: M = Co, Ni), and $[(\eta^6\text{-C}_6\text{H}_6)\text{NiPH}_3]$ (D). Keeping the metal–ligand distances constant when changing the metal atom allows for a better comparison on the effect of the metal center. The actual geometric parameters employed in the calculations were as follows (see also the drawings for A–D): M– C_6H_6 (centroid) = 1.70 Å; M– $\text{C}(\eta^6\text{-C}_6\text{H}_6)$ = 2.20 Å; M– C_5H_5 (centroid) = 1.73 Å; M– $\text{C}(\eta^5\text{-C}_5\text{H}_5)$ = 2.10 Å; M– $\text{C}(\sigma\text{-C}_6\text{F}_5)$ = 1.90 Å; Ni–P = 2.10 Å; C– $\text{C}(\eta^5\text{-C}_5\text{H}_5)$ = 1.40 Å; C– $\text{C}(\eta^6\text{-C}_6\text{H}_6)$ = 1.39 Å; C– $\text{C}(\text{C}_6\text{F}_5, \text{bipy})$ = 1.40 Å; C–H = 1.05 Å; C–F = 1.35 Å. The distances of M– $\text{C}(\eta^6\text{-arene})$ found in the X-ray structures lie within 0.15 Å of the 2.20 Å assumed for M– $\text{C}(\eta^6\text{-C}_6\text{H}_6)$ with M = V, Co, and Ni. The atomic parameters used were taken from established work and are listed in Table 2.

Horizontal ionization energy calculations were performed with the HyperChem computational package (Version 5.0, Hypercube Inc., Waterloo, Ontario, Canada). Geometry optimizations were carried out on the model complex $[(\eta^5\text{-Cp})\text{Ni}(\text{C}_6\text{H}_4\text{-N=N-C}_6\text{H}_5\text{-}\kappa\text{C},\kappa\text{N})]$ **A** with the ZINDO/1 method. The Ni– C_{aryl} and Ni–N contacts were refined free to values of Ni– C^{19} = 1.956 Å and Ni– N^1 = 1.949 Å. For comparison these values were also restrained to the experimental bond lengths of Ni– C^{19} = 1.864 and Ni– $\text{N} = 1.816\text{ Å}$. In addition, the bond angle $\text{C}^{12}\text{-N}^1\text{-N}^2$ was restrained to 113° . No other restrictions were applied. Single-point LCAO–MO–SCF calculations using the ZINDO/S approxi-

Table 2. Parameters used in the Extended Hückel Calculations

	Orbital	Energy H_{ii}/eV	Exponents		Coefficients		Ref.
			ζ_1	ζ_2	c_1	c_2	
Ni	3d	-12.99	5.75	2.00	0.5682	0.6292	[33]
	4s	-8.86	2.1				
	4p	-4.90	2.1				
Co	3d	-13.180	5.55	2.10	0.5679	0.6059	[45]
	4s	-9.21	2.0				
	4p	-5.29	2.0				
Fe	3d	-12.700	5.35	1.80	0.5366	0.6678	[45]
	4s	-9.17	1.9				
	4p	-5.37	1.9				
V	3d	-11.000	4.75	1.70	0.4755	0.7052	[46]
	4s	-8.81	1.3				
	4p	-5.52	1.3				
C	2s	-21.4	1.625				[a]
	2p	-11.4	1.625				
F	2s	-40.0	2.425				[a]
	2p	-18.1	2.425				
P	2s	-18.6	1.6				[a]
	2p	-14.0	1.6				
H	1s	-13.6	1.3				[a]

[a] As given in parameter file of the CACAO program; standard EH parameters.

mation with spectroscopic parameterization^[24] have been performed on the model complex **A** in its respective ZINDO/1 optimized geometry. The restraints did not lead to large changes in orbital composition or energetic order.

Synthesis

[(η^5 -Me₄EtC₅)Ni]₂(μ - η^3 : η^3 decacyclene) (3): Decacyclene (250 mg, 0.6 mmol) was suspended in 50 mL of THF and transferred into a flask in which a metallic mirror from 60 mg (1.54 mmol) of potassium metal had been prepared. After 3 d, ca. 90% of the metal was dissolved, resulting in a deep red-brown solution. After cooling to -78 °C, [(η^5 -Me₄EtC₅)Ni(η^2 -acac)]^[47] (**1**) (370 mg, 1.2 mmol) was added to this solution in one batch under stirring, and the resulting mixture was allowed to warm to room temperature during several hours. After removal of all volatiles, the residue was dissolved in diethyl ether and crystallized from that solvent at -30 °C, resulting in 360 mg (0.42 mmol, 74%) of shimmering black crystals of **3**. - ¹H NMR (300 MHz, C₆D₆): δ = 0.52 (t, 6 H), 0.77 (s, 12 H), 0.78 (s, 12 H), 1.27 (q, 4 H), 7.42 (t, ³J = 7.2 Hz, 6 H), 7.63 (d, ³J = 7.2 Hz, 6 H), 8.36 (t, ³J = 7.2 Hz, 6 H). - ¹³C NMR (75 MHz, C₆D₆): δ = 7.8, 7.9, 14.6, 16.7, 97.5, 98.9, 104.6, 118.9, 123.2, 132.2, 135.9, 142.9. - IR (KBr): $\tilde{\nu}$ = 3048, 2963, 2925, 2857, 1581, 1482, 1457, 1435, 1378, 1355, 1301, 819, 800, 771, 758 cm⁻¹. - C₅₈H₅₂Ni₂ (866.47): calcd. C 80.40, H 6.05; found C 81.00, H 6.38.

The general experimental procedure for reactions of **3** with the dichalcogenides **5–8** was as follows: To solution of the dichalcogenide in diethyl ether at 0 °C a diethyl ether solution of **3** was added. Upon warming to ambient temperature precipitation of tan colored decacyclene occurred. The resulting mixture was reduced in volume and filtered through Celite. Crystallization at -30 °C afforded complexes **9–12**.

[(η^5 -Me₄EtC₅)Ni]₂(μ -SPh)₂ (9): Brown crystals; yield: 300 mg (0.4 mmol, 84%). - ¹H NMR (300 MHz, C₆D₆): δ = 0.91 (t, 6 H), 1.13 (s, 12 H), 1.20 (s, 12 H), 1.85 (q, 4 H), 7.02 (m, 6 H), 8.36 (m, 4 H). - ¹³C NMR (75 MHz, C₆D₆): δ = 8.9, 9.0, 14.3, 17.9, 97.6, 99.0, 99.3, 106.9, 125.3, 127.5, 136.1, 138.9. - MS (EI): m/z (%) = 632 (60) [M⁺], 316 (100) [M⁺/2]. - IR (KBr): $\tilde{\nu}$ = 3059, 2961, 2903, 2854, 1576, 1473, 1450, 1436, 1378, 1347, 1297, 1262, 1153, 1022, 819, 769, 738, 689 cm⁻¹. - C₃₄H₄₄Ni₂S₂ (634.266): calcd. C 64.39, H 6.99, S 10.11; found C 67.08, H 6.65, S 7.43.

[(η^5 -Me₄EtC₅)Ni]₂(μ -SeMes)₂ (10): Brown microcrystals; yield: 360 mg (0.4 mmol, 79%). - ¹H NMR (300 MHz, C₆D₆): δ = 0.80 (t, 6 H), 1.23 (s, 24 H), 1.86 (q, 4 H), 2.11 (s, 6 H), 2.55 (s, 6 H) broad, 4.33 (s, 6 H) broad, 6.70 (s, 2 H) broad, 6.99 (s, 2 H) broad. - ¹³C NMR (75 MHz, C₆D₆): δ = 9.1, 9.2, 14.2, 18.0, 21.0, 98.6, 105.5, 120.1, 135.0. - MS (EI): m/z (%) = 812 (20) [M⁺], 406 (100) [M⁺/2]. - C₄₀H₅₆Ni₂Se₂ (812.228): calcd. C 59.15, H 6.95; found C 54.72, H 6.72.

[(η^5 -Me₄EtC₅)Ni]₂(μ -TeMes)₂ (11): Brown microcrystals; yield: 410 mg (0.4 mmol, 80%). - ¹H NMR (300 MHz, C₆D₆): δ = 0.83 (t, 6 H), 1.50 (s, 12 H), 1.52 (s, 6 H), 1.53 (s, 6 H), 2.03 (q, 4 H), 2.10 (s, 6 H), 2.70 (s, 6 H), 3.62 (s, 6 H), 6.68 (s, 2 H), 6.86 (s, 2 H). - ¹³C NMR (75 MHz, C₆D₆): δ = 9.9, 10.0, 10.1, 10.2, 15.1, 18.9, 21.0, 29.9, 32.1, 98.1, 98.3, 99.4, 99.7, 104.8, 126.4, 127.0, 136.4, 144.6, 146.0. - MS (EI): m/z (%) = 910 (15) [M⁺], 791 (17) [M⁺ - mesitylene], 456 (18) [M⁺/2], 119 (100) [mesitylene]. - C₄₀H₅₆Ni₂Te₂ (909.508): calcd. C 52.82, H 6.21; found C 53.10, H 6.18.

[(η^5 -Me₄EtC₅)Ni]₂(μ -TeNaphth)₂ (12): Black crystals; yield: 380 mg (0.4 mmol, 73%). - ¹H NMR (300 MHz, C₆D₆): δ = 0.75 (t, 6 H), 1.38 (s, 12 H), 1.40 (s, 6 H), 1.41 (s, 6 H), 1.92 (q, 4 H), 7.05 (t, ³J = 7.7 Hz, 2 H), 7.30 (m, 2 H), 7.45 (m, 2 H), 7.55 (d, ³J = 8.1 Hz, 2 H), 7.61 (d, ³J = 7.7 Hz, 2 H), 8.81 (d, ³J = 7.7 Hz, 2 H), 9.38 (d, ³J = 8.1 Hz, 2 H). - ¹³C NMR (75 MHz, C₆D₆): δ = 10.1, 10.2, 10.3, 10.4, 15.3, 19.0, 98.5, 99.0, 99.9, 100.5, 100.7, 105.8, 125.3, 126.0, 126.1, 128.8, 132.8, 133.0, 138.4, 141.9. - MS (EI): m/z (%) = 926 (15) [M⁺], 799 (10) [M⁺ - naphthalene], 464 (15) [M⁺/2], 253 (100) [binaphthalene]. - C₄₂H₄₈Ni₂Te₂ (925.466): calcd. C 54.51, H 5.23; found C 55.05, H 5.36.

[(η^5 -Me₄EtC₅)Ni(C₆H₄-N=N-C₆H₅- κ C, κ N)] (13): This compound was prepared by adding a stoichiometric amount of azobenzene to a solution of **3** in 500 mL of diethyl ether at room temperature. While stirring for 12 h, the color changed from brown red to deep blue. Crystallization from diethyl ether afforded dark blue crystals; yield: 380 mg (1.0 mmol, 88%). - ¹H NMR (300 MHz, CD₂Cl₂): δ = 0.93 (t, 3 H), 1.62 (s, 6 H), 1.73 (s, 6 H), 2.15 (q, 2 H), 7.08 (m, 1 H, C⁵-H), 7.13 (m, 1 H, C⁴-H), 7.16 (m, 2 H, C^{8,8'}-H), 7.37 (m, 1 H, C¹⁰-H), 7.47 (m, 2 H, C^{9,9'}-H), 7.86 (m, 1 H, C³-H), 8.11 (m, 1 H, C⁶-H). - ¹³C NMR (75 MHz, CD₂Cl₂): δ = 9.3, 9.5, 15.1, 17.7, 100.4, 101.4, 108.2 [(η^5 -Me₄EtCp)Ni], 123.0 (C^{8,8'}), 123.2 (C⁴), 123.8 (C⁵), 127.5 (C¹⁰), 127.6 (C⁶), 128.8 (C⁹), 138.5 (C³), 157.4 (C⁷), 163.1 (C¹), 181.9 (C²). - MS (EI): m/z (%) = 388 (100) [M⁺]. - IR (KBr): $\tilde{\nu}$ = 3082, 3055, 3039, 2961, 2912, 2867, 1588, 1567, 1484, 1447, 1296, 1287, 1262, 1032, 1017, 770, 753, 711, 698 cm⁻¹. - UV/Vis (CH₂Cl₂): λ_{max} (ϵ) = 230 (24923), 250 (21760), 300 (25237), 345 (9203), 510 (3243), 609 nm (6317). - C₂₃H₂₆N₂Ni (389.18): calcd. C 70.98, H 6.73, N 7.20; found C 70.31, H 6.98, N 6.89.

[(η^5 -C₅Me₅)Ni(C₆H₄-N=N-C₆H₅- κ C, κ N)] (14): As with the synthesis of **13**. Blue, needle-like crystals, prepared from **4**; yield: 350 mg (0.9 mmol, 85%). - ¹H NMR (300 MHz, C₆D₆): δ = 1.50 (s, 15 H) 7.0 (m, 1 H, C¹⁰-H), 7.06–7.22 (m, 6 H), 7.94 (dd, ³J =

7.9 Hz, $^4J = 1.1$ Hz, 1 H, C³-H), 8.50 (dd, $^3J = 7.7$ Hz, $^4J = 1.5$ Hz, 1 H, C⁶-H). – ^{13}C NMR (75 MHz, C₆D₆): $\delta = 9.4, 100.6, 123.2, 123.7, 124.0, 127.1, 138.4, 157.7, 164.1, 182.7$. – MS (EI): m/z (%) = 374 (100) [M⁺]. – IR (KBr): $\tilde{\nu} = 3058, 3039, 2979, 2952, 2898, 2851, 1589, 1484, 1420, 1385, 1297, 1263, 1154, 1068, 1017, 769, 758, 753, 711, 698$ cm⁻¹. – C₂₂H₂₄N₂Ni (375.16): calcd. C 70.44, H 6.45, N 7.47; found C 64.17, H 5.99, N 6.95. Although this analysis was repeated several times with recrystallized material, C,H,N values for **15** were repeatedly unsatisfactorily.

[(η^5 -C₅H₅)Fe[μ -(η^5 -C₅H₃CH₂NMe₂- κ C, κ N)]Ni(η^5 -C₅EtMe₄)] (**16**): Solid **3** (180 mg, 0.2 mmol) was added to a yellow suspension of plumblylene **15** (140 mg, 0.2 mmol) in diethyl ether at -78 °C. Within a few hours precipitation of decacyclene (**2**) occurred and the color of the solution turned to purple, while upon warming to ambient temperature it changed to red-brown. The mixture was reduced in volume and filtered through Celite. Crystallization at -78 °C afforded 60 mg (0.1 mmol, 65%) of complex **16** as red to black crystals. – ^1H NMR (300 MHz, C₆D₆): $\delta = 1.11$ (t, 3 H), 1.69 (s, 3 H), 1.70 (s, 3 H), 1.72 (s, 6 H), 1.86 [s, 3 H, N(CH₃)₂], 2.24 (q, 2 H), 2.33 [s, 3 H, N(CH₃)₂], 2.59 (d, $^2J = 13.6$ Hz, 1 H, Fc-CH₂), 2.89 (d, $^2J = 13.6$ Hz, 1 H, Fc-CH₂), 3.84 (d, $^3J = 2.1$ Hz, 1 H, C₅H₃Fe), 3.98 (d, $^3J = 2.1$ Hz, 1 H, C₅H₃Fe), 4.20 (s, 5 H, C₅H₅Fe), 4.24 (t, $^3J = 2.1$ Hz, 1 H, C₅H₃Fe). – ^{13}C NMR (75 MHz, C₆D₆): $\delta = 10.4, 10.5, 15.2, 19.2, 53.2$ [N(CH₃)₂], 53.4 [N(CH₃)₂], 60.8 (C₅H₃Fe), 66.5 (C⁴), 68.4 (Fc-CH₂), 69.1 (C₅H₅Fe), 71.7 (C₅H₃Fe), 90.2 (C¹), 92.4 (C²), 95.5, 96.1, 97.2, 97.4, 103.8. – MS (EI): m/z (%) = 449 (100) [M⁺], 326 (45) [M⁺ - C₅H₃Fe], 242 (20) [M⁺ - C₁₁H₁₇Ni]. – IR (KBr): $\tilde{\nu} = 3079, 3026, 2961, 2922, 2852, 2769, 1451, 1415, 1383, 1353, 1302, 1227, 1158, 1105, 1043, 1022, 974, 947, 864, 846, 809, 795$ cm⁻¹. – C₂₄H₃₃FeNNi (450.09): calcd. C 64.05, H 7.39, N 3.11; found C 57.89, H 6.96, N 3.11. Probably due to excess [(dimethylamino)methyl]ferrocene that could not be removed completely by washing without dissolving most of **16**, the C value is found out of the usually acceptable range.

Acknowledgments

The work of J. J. S. was supported by the DFG (Heisenberg fellowship to J. J. S.), by the Stiftung Volkswagenwerk and the Fonds der Chemischen Industrie which is acknowledged with gratitude. We are grateful to the mass spectrometric department of the MPI für Kohlenforschung, Mülheim, for recording the mass spectra and Mr. K. Kowski, University of Essen, for recording the PE spectrum of **13**. The work of C. J. was supported by the DFG and the Fonds der Chemischen Industrie. A copy of the CACAO program was kindly provided by Dr. D. M. Proserpio.

- [1] J. J. Schneider, D. Spickermann, T. Labahn, J. Magull, M. Fontani, F. Laschi, P. Zanello, *Chem. Eur. J.* **2000**, *6*, 3686.
 [2] [2a] M. Munakata, L. P. Wu, G. L. Ning, T. Kuroda-Sowa, M. Maekawa, Y. Suenaga, N. Maeno, *J. Am. Chem. Soc.* **1999**, *121*, 4968. – [2b] T. Kubo, K. Yamamoto, K. Nakasuji, T. Takui, I. Murata, *Angew. Chem.* **1996**, *108*, 456; *Angew. Chem. Int. Ed. Engl.* **1996**, *35*, 439. – [2c] K. Zimmermann, R. Goddard, C. Krüger, M. W. Haenel, *Tetrahedron Lett.* **1996**, *37*, 8371. – [2d] K. Zimmermann, M. W. Haenel, *Synlett* **1997**, 609.
 [3] [3a] J. Edwin, M. Bochmann, M. C. Böhm, D. E. Brennan, W. E. Geiger, C. Krüger, J. Pebler, H. Pritzkow, W. Siebert, W. Swiridoff, H. Wadepohl, J. Weiss, U. Zenneck, *J. Am. Chem. Soc.* **1983**, *105*, 2582. – [3b] W. Siebert, *Angew. Chem.* **1985**, *97*, 924; *Angew. Chem. Int. Ed. Engl.* **1985**, *24*, 943. – [3c] H. Werner, *Angew. Chem. Int. Ed. Engl.* **1977**, *89*, 1; *Angew. Chem. Int. Ed. Engl.* **1977**, *16*, 1. – [3d] G. E. Herberich, H. Ohst, *Adv. Organomet. Chem.* **1986**, *25*, 199. – [3e] G. E. Herberich in *Comprehensive Organometallic Chemistry* (Eds.: E. W. Abel, F. G. A. Stone, G. Wilkinson), Pergamon Press, Oxford, **1982**, vol. 1, chapter 5,

- p. 197. – [3f] P. Greiwe, M. Sabat, R. N. Grimes, *Organometallics* **1995**, *14*, 3683. – [3g] R. N. Grimes, *Coord. Chem. Rev.* **1979**, *28*, 47. – [3h] X. Wong, M. Sabat, R. N. Grimes, *J. Am. Chem. Soc.* **1995**, *117*, 12227.
 [4] X-ray crystallographic investigations on **3**, **9**, and **16**. – **3**: Formula C₅₈H₅₂Ni₂, $M = 866.42$; crystal dimensions $0.21 \times 0.16 \times 0.12$ mm, black, measured with a Siemens SMART-CCD diffractometer (three-axis platform) with Mo- K_{α} radiation at 293(2) K. Cell dimensions $a = 13.6342(10)$, $b = 16.8886(12)$, $c = 18.6494(13)$ Å, $V = 4294.3(5)$ Å³; orthorhombic crystal system, $Z = 4$, $d_{\text{calcd.}} = 1.340$ gcm⁻³, $\mu = 0.917$ mm⁻¹, space group $Pca2_1$, data collection of 34489 intensities ($2\theta_{\text{max}} = 50^\circ$, 0.3° ω -scans 120 frames at $\phi = 0^\circ$, four runs 0.3° ϕ -scans with 600 frames at angles 135, 143, 156 and 169° in ω , more than 97% of the data covered), absorption correction with Siemens SADABS (R_{merge} before/after 0.1414/0.0426, max/min equivalent transmission 1.00/0.59), 10428 independent and 6167 “observed” data [$F_{\sigma} \geq 4\sigma(F)$], structure solution with direct methods (Siemens SHELXTL-Plus Vers. 5.03) and refined on F^2 (Siemens SHELXL-97) (541 parameters). Hydrogen atom positions were calculated and refined as riding groups with the 1.2-fold (1.5 for methyl groups) isotropic U values. $R1 = 0.0505$, $wR2 = 0.1032$, $w^{-1} = \sigma^2(F_{\sigma}^2) + (0.0592 \cdot P)^2$, where $P = [(max(F_{\sigma}^2) + (2F_{\sigma}^2) \cdot 0.311 \text{ eÅ}^{-3}) \text{ close to the heavy atoms.} - \mathbf{9}$: Formula C₃₄H₄₄Ni₂S₂, $M = 634.23$, $a = 10.6922(5)$ Å, $b = 11.9271(6)$ Å, $c = 14.0125(7)$ Å, $\alpha = 84.307(3)^\circ$, $\beta = 75.012(3)^\circ$, $\gamma = 63.581(2)^\circ$, $V = 1545.64(13)$ Å³, $d_{\text{calcd.}} = 1.363$ gcm⁻³, $\mu = 1.375$ mm⁻¹, empirical absorption correction with SADABS^[a], $Z = 2$, two half-independent molecules in the asymmetric unit (bond parameters identical within esds), triclinic, space group $P1$, $\lambda = 0.71073$ Å, $T = 133(2)$ K, 15845 reflections collected, 4048 independent and 3695 observed reflections [$I \geq 2\sigma(I)$], 353 parameters, $R = 0.0619$, $wR_2 = 0.1108$, max/min residual electron density: $0.339/-0.694$ e Å⁻³, position of the hydrogen atoms calculated and riding. G. M. Sheldrick, SADABS, **1999**; computer program for correction of diffractometer data, Universität Göttingen. – **16**: Formula C₂₄H₃₃FeNNi, $M = 450.07$; crystal dimensions $0.28 \times 0.26 \times 0.12$ mm, dark brown block, measured with a Siemens SMART-CCD diffractometer (three-axis platform) with Mo- K_{α} radiation at 203(2) K. Cell dimensions $a = 9.6053(8)$, $b = 8.6511(7)$, $c = 25.522(2)$ Å, $\beta = 90.445(2)^\circ$, $V = 2111.2(3)$ Å³; monoclinic crystal system, $Z = 4$, $d_{\text{calcd.}} = 1.416$ gcm⁻³, $\mu = 0.917$ mm⁻¹, space group $P2_1/n$, data collection of 5568 intensities ($2\theta_{\text{max}} = 50^\circ$, 0.3° ω -scans 120 frames at $\phi = 0^\circ$, four runs 0.3° ϕ -scans with 636 frames at angles 0.88, 180, 270° in ω , more than 99% of the data covered), absorption correction with Bruker AXS SADABS (R_{merge} before/after 0.0626/0.0485, max/min equivalent transmission 1.00/0.81), 5218 independent and 3610 “observed” data [$F_{\sigma} \geq 4\sigma(F)$], structure solution with direct methods (Bruker AXS SHELXTL-Plus Vers. 5.10 DOS/WIN95/NT) and refined on F^2 (SHELXL-97) (244 parameters). Hydrogen atom positions were calculated and refined as riding groups with the 1.2-fold (1.5 for methyl groups) isotropic U values. $R1 = 0.0453$, $wR2 = 0.1013$, $w^{-1} = \sigma^2(F_{\sigma}^2) + (0.068 \cdot P)^2$, where $P = [(F_{\sigma}^2) + (2F_{\sigma}^2)]/3$, $\text{GOF} = 0.974$, max/min residual electron density $1.522/-0.312$ eÅ⁻³ close to the heavy atoms. – Crystallographic data (excluding structure factors) for the structures reported in this paper have been deposited with the Cambridge Crystallographic Data Centre as supplementary publication nos. CCDC-141845 (**3**), -139245 (**9**), and -141844 (**16**). Copies of the data can be obtained free of charge on application to CCDC, 12 Union Road, Cambridge CB2 1EZ, UK [Fax: (internat.) + 44-1223/336-033; E-mail: deposit@ccdc.cam.ac.uk].
 [5] [5a] J. Müller, P. Escarpa Gaede, K. Qiao, *Angew. Chem.* **1993**, *105*, 1809; *Angew. Chem. Int. Ed. Engl.* **1993**, *32*, 1697. – [5b] J. Müller, P. Escarpa Gaede, K. Qiao, *J. Organomet. Chem.* **1994**, *480*, 213. – [5c] J. J. Schneider, U. Specht, R. Goddard, C. Krüger, J. Ensling, P. Gülich, *Chem. Ber.* **1995**, *128*, 941. – [5d] J. J. Schneider, D. Wolf, U. Denninger, R. Goddard, C. Krüger, *J. Organomet. Chem.* **1999**, *579*, 139.
 [6] K. Jonas, G. Koepe, L. Schieferstein, R. Mynott, C. Krüger, Y.-H. Tsay, *Angew. Chem.* **1983**, *95*, 637; *Angew. Chem. Int. Ed. Engl.* **1983**, *22*, 620; *Angew. Chem. Suppl.* **1983**, 920.
 [7] W. J. Evans, S. L. Gonzales, J. W. Ziller, *J. Am. Chem. Soc.* **1994**, *116*, 2600.
 [8] J. J. Schneider, D. Wolf, U. Denninger, R. Goddard, C. Krüger, *J. Organomet. Chem.* **1999**, *579*, 139.

- [9] I. Bach, K.-R. Pörschke, R. Goddard, C. Kopske, C. Krüger, A. Rufinska, K. Seevogel, *Organometallics* **1996**, *15*, 4959 and ref. cited therein.
- [10] D. M. Ho, R. A. Pascal, Jr., *Chem. Mater.* **1993**, *5*, 1358.
- [11] [11a] N. Tokitoh, Y. Matsuhashi, R. Okazaki, *Organometallics* **1993**, *12*, 2894. — [11b] Y. Matsuhashi, N. Tokitoh, R. Okazaki, *Organometallics* **1994**, *13*, 4387. — [11c] K. Merzweiler, L. Weise, *Z. Naturforsch., Teil B* **1990**, *45*, 971. — [11d] K. Merzweiler, H. Kraus, *Z. Naturforsch., Teil B* **1997**, *52*, 635. [11e] K. Merzweiler, H. Kraus, L. Weise, *Z. Naturforsch., Teil B* **1993**, *48*, 287. —
- [12] [12a] N.-F. Ho, T. C. W. Mak, T.-Y. Luh, *J. Chem. Soc., Dalton Trans.* **1990**, 3591–3595. — [12b] R. E. Dessy, R. Kornmann, C. Smith, R. Haytor, *J. Am. Chem. Soc.* **1968**, *80*, 2001. — [12c] R. E. Dessy, L. Wiczorek, *J. Am. Chem. Soc.* **1969**, *91*, 4963.
- [13] [13a] J. J. Schneider, N. Czap, D. Bläser, R. Boese, *J. Am. Chem. Soc.* **1999**, *121*, 1409. — [13b] J. J. Schneider, J. Hagen, D. Spickermann, D. Bläser, R. Boese, F. F. de Biani, F. Laschi, P. Zanello, *Chem. Eur. J.* **2000**, *6*, 237.
- [14] G. Aullón, G. Ujaque, A. Lledós, S. Alvarez, *Chem. Eur. J.* **1999**, *5*, 1391.
- [15] *Handbook of Chemistry and Physics*, 61th ed., CRC Press, Boca Raton, Florida, **1980**, F219.
- [16] [16a] A. D. Ryabov, *Chem. Rev.* **1990**, *90*, 403. — [16b] M. Ghedini, D. Pucci, A. Crispini, G. Barberio, *Organometallics* **1999**, *18*, 2116.
- [17] [17a] N. L. Cromhout, J. F. Gallagher, A. R. Manning, A. Paul, *Organometallics* **1999**, *18*, 1119. — [17b] N. Gül, J. H. Nelson, *Organometallics* **1999**, *18*, 709. — [17c] S. Attar, J. H. Nelson, J. Fischer, A. de Cian, J. P. Sutter, M. Pfeffer, *Organometallics* **1995**, *14*, 4559. — [17d] Z.-X. Wang, C.-S. Jia, Z.-Y. Zhou, X.-G. Zhou, *J. Organomet. Chem.* **1999**, *580*, 201. — [17e] V. I. Sokolov, L. L. Troitskaya, O. A. Reutov, *J. Organomet. Chem.* **1999**, *580*, 201. — [17f] K. G. Gaw, A. M. Z. Slawin, M. B. Smith, *Organometallics* **1999**, *18*, 3255.
- [18] [18a] J. Kleimann, M. Dubbeck, *J. Am. Chem. Soc.* **1963**, *85*, 1544. — [18b] D. Sutton, *Chem. Rev.* **1993**, *93*, 995.
- [19] A. C. Cope, R. W. Siekman, *J. Am. Chem. Soc.* **1965**, *87*, 3272.
- [20] [20a] H. Takahashi, J. Tsuji, *J. Organomet. Chem.* **1967**, *10*, 511. — [20b] M. I. Bruce, B. C. Godall, F. G. A. Stone, *J. Chem. Soc., Chem. Commun.* **1973**, 558. — [20c] M. I. Bruce, B. C. Godall, F. G. A. Stone, *J. Chem. Soc., Dalton Trans.* **1987**, 687. — [20d] A. K. Yatsimirsky, *Zh. Neorg. Khim.* **1979**, *24*, 2711. — [20e] R. F. Heck, *J. Am. Chem. Soc.* **1968**, *90*, 313.
- [21] [21a] P. L. Watson, *J. Chem. Soc., Chem. Commun.* **1983**, 276. — [21b] B. J. Dellman, W. M. Stevels, J. H. Teuben, M. T. Lakin, A. L. Spek, *Organometallics* **1994**, *13*, 3881. — [21c] J. J. Schneider, *Chem. Ber.* **1995**, *128*, 321.
- [22] [22a] K. Kokkinos, R. Wizinger, *Helv. Chim. Acta* **1971**, *54*, 330. — [22b] W. I. Cross, K. R. Flower, R. G. Pritchard, *J. Organomet. Chem.* **2000**, *601*, 164.
- [23] [23a] J. J. Schneider, U. Denninger, O. Heinemann, C. Krüger, *Angew. Chem.* **1995**, *107*, 631; *Angew. Chem. Int. Ed. Engl.* **1995**, *34*, 592. — [23b] J. J. Schneider, D. Wolf, C. Janiak, O. Heinemann, J. Rust, C. Krüger, *Chem. Eur. J.* **1998**, *4*, 1982. — [23c] J. J. Schneider, D. Wolf, *Z. Naturforsch., Teil B* **1998**, *53*, 1.
- [24] [24a] M. C. Zerner, G. H. Loew, R. F. Kirchner, U. T. Mueller-Westerhoff, *J. Am. Chem. Soc.* **1980**, *102*, 589. — [24b] A. D. Bacon, M. C. Zerner, *Theor. Chim. Acta* **1979**, *53*, 21. — [24c] M. C. Zerner in *Reviews in Computational Chemistry II* (Eds.: K. B. Lipkowitz, D. B. Boyd), VCH, Weinheim, **1991**, p. 313.
- [25] T. Koopmans, *Physica* **1934**, *104*, 1.
- [26] M. C. Böhm, *Z. Naturforsch., Teil A* **1982**, *37*, 1193 and refs. therein.
- [27] C. Janiak, N. Kuhn, R. Gleiter, *J. Organomet. Chem.* **1994**, *475*, 223.
- [28] [28a] J. J. Schneider, N. Czap, *J. Chem. Soc., Dalton Trans.* **1999**, 595. — [28b] J. J. Schneider, N. Czap, D. Bläser, R. Boese, *J. Am. Chem. Soc.* **1999**, *121*, 1409. — [28c] J. J. Schneider, N. Czap, D. Bläser, R. Boese, *J. Organomet. Chem.* **1999**, *584*, 338. — [28d] J. J. Schneider, J. Hagen, N. Czap, C. Krüger, S. A. Mason, R. Bau, J. Ensling, P. Gütlich, B. Wrackmeyer, *Chem. Eur. J.* **2000**, *6*, 625. [28e] J. J. Schneider, N. Czap, D. Bläser, R. Boese, J. Ensling, P. Gütlich, C. Janiak, *Chem. Eur. J.* **2000**, *6*, 468.
- [29] [29a] N. Davidovic, K. Jacob, A. H. van der Zeijden, H. Menge, K. Merzweiler, C. Wagner, *Organometallics* **2000**, *19*, 1438. — [29b] J. J. Schneider, *Nachr. Chem.* **2000**, *5*, 614.
- [30] M. R. Meneghetti, M. Grellier, M. Pfeffer, J. Dupont, J. Fischer, *Organometallics* **1999**, *18*, 5560.
- [31] [31a] A. W. Duff, K. Jonas, R. Goddard, H.-J. Kraus, C. Krüger, *J. Am. Chem. Soc.* **1983**, *105*, 5479. — [31b] K. Jonas, *Angew. Chem.* **1985**, *97*, 292; *Angew. Chem. Int. Ed. Engl.* **1985**, *24*, 295.
- [32] [32a] L. J. Radonovich, M. W. Eyring, T. J. Groshens, K. J. Klabunde, *J. Am. Chem. Soc.* **1982**, *104*, 2816. — [32b] K. J. Klabunde, B. B. Anderson, M. Bader, L. J. Radonovich, *J. Am. Chem. Soc.* **1978**, *100*, 1313. — [32c] L. J. Radonovich, K. J. Klabunde, C. B. Behrens, D. P. McCollar, B. B. Anderson, *Inorg. Chem.* **1980**, *178*, 197. — [32d] R. G. Gastinger, K. J. Klabunde, *Trans. Met. Chem.* **1979**, *4*, 1.
- [33] L. J. Radonovich, F. J. Koch, T. A. Albright, *Inorg. Chem.* **1980**, *19*, 3373.
- [34] T. Nickel, R. Goddard, C. Krüger, K.-R. Pörschke, *Angew. Chem.* **1994**, *106*, 908; *Angew. Chem. Int. Ed. Engl.* **1994**, *33*, 879.
- [35] J. W. Lauher, M. Elian, R. H. Summerville, R. Hoffmann, *J. Am. Chem. Soc.* **1976**, *98*, 3219.
- [36] W. Tremel, R. Hoffmann, M. Kertesz, *J. Am. Chem. Soc.* **1989**, *111*, 2030.
- [37] L. J. Radonovich, M. W. Eyring, T. J. Groshens, K. J. Klabunde, *J. Am. Chem. Soc.* **1982**, *104*, 2816.
- [38] P. T. Chesky, M. B. Hall, *J. Am. Chem. Soc.* **1984**, *106*, 5186.
- [39] T. A. Albright, J. K. Burdett, M.-H. Whangbo, *Orbital Interactions in Chemistry*, Wiley-Interscience, New York, **1985**. R. Hoffmann, *Solids and Surfaces: A Chemists View of Bonding in Extended Structures*, VCH, Weinheim, **1988**.
- [40] C. Janiak, R. Hoffmann, *J. Am. Chem. Soc.* **1990**, *112*, 5924.
- [41] M. Akiba, M. V. Lakshminantham, K.-Y. Jen, M. P. Cava, *J. Org. Chem.* **1984**, *49*, 4819.
- [42] R. Hoffmann, *J. Chem. Phys.* **1963**, *39*, 1397–1412. R. Hoffmann, W. N. Lipscomb, *J. Chem. Phys.* **1962**, *36*, 2179–2189. R. Hoffmann, W. N. Lipscomb, *J. Chem. Phys.* **1962**, *37*, 2872.
- [43] J. H. Ammeter, H.-B. Bürgi, J. C. Thibeault, R. Hoffmann, *J. Am. Chem. Soc.* **1978**, *100*, 3686–3692.
- [44] C. Mealli, D. M. Proserpio, *J. Chem. Educ.* **1990**, *67*, 399.
- [45] R. H. Summerville, R. Hoffmann, *J. Am. Chem. Soc.* **1976**, *98*, 7240.
- [46] P. Kubáček, R. Hoffmann, Z. Havlas, *Organometallics* **1982**, *1*, 180.
- [47] E. E. Bunel, L. Valle, J. M. Manriquez, *Organometallics* **1985**, *4*, 1680.

Received June 16, 2000

[100244]